

# Half-metallic graphene nanodots

Oded Hod<sup>1</sup>, Verónica Barone<sup>2</sup>, and Gustavo E. Scuseria<sup>1</sup>

<sup>1</sup>*Department of Chemistry, Rice University, Houston, Texas 77005-1892;*

<sup>2</sup>*Department of Physics, Central Michigan University, Mt. Pleasant, MI 48859*

(Dated: February 1, 2008)

A comprehensive *first-principles* theoretical study of the electronic properties and half-metallic nature of finite rectangular graphene nanoribbons is presented. We identify the bisanthrene isomer of the  $C_{28}H_{14}$  molecule to be the smallest polycyclic aromatic hydrocarbon to present a spin polarized ground state. Even at this quantum dot level, the spins are predicted to be aligned anti-ferromagnetically at the two zigzag edges of the molecule. As a rule of thumb, we find that zigzag edges that are at least three consecutive units long, will present spin polarization if the width of the system is 1 nm or wider. Room temperature detectability of the magnetic ordering is predicted for molecules with zigzag edges 1 nm and longer. For the longer systems studied, spin wave structures appear in some high spin multiplicity states. Energy gap oscillations with the length of the zigzag edge are observed. The amplitude of these oscillations is found to be smaller than that predicted for infinite ribbons. The half-metallic nature of the ribbons under an external in-plane electric field is found to be preserved even for finite and extremely short systems.

Since their recent successful fabrication,<sup>1</sup> graphene nanoribbons (GNRs) have been the focus of extensive experimental and theoretical efforts. GNRs have the same unique hexagonal carbon lattice as carbon nanotubes (CNTs), confined to a quasi-one-dimensional structure. Hence, they share a variety of interesting physical characteristics. Experimental evidence of ballistic electronic transport, large phase coherence lengths, and current density sustainability,<sup>2</sup> accompanied by theoretical predictions and experimental verification of interesting magnetic properties<sup>3,4,5,6,7,8,9</sup>, quasi-relativistic behavior,<sup>10,11,12,13</sup> and bandgap engineering capabilities<sup>14,15,16,17</sup> mark GNRs as potential building blocks in future nanoelectronic devices. Furthermore, due to their planar geometry, standard lithographic techniques may be used for the flexible design of a variety of experimental devices<sup>1,2,10,13,17</sup> in a controllable and reproducible manner.

Despite the aforementioned similarities, there is a distinct difference between CNTs and GNRs. Unlike the tubular shaped nanotubes, GNRs, which are long and narrow strips cut out of a two dimensional graphene sheet, present long and reactive edges prone to localization of electronic states. The importance of these edge states was demonstrated for the case of armchair CNTs which present a metallic and non-magnetic<sup>18,19</sup> character in their tubular form, but when unrolled into the corresponding zigzag GNRs, they were predicted to become semiconducting<sup>9,20</sup> with a spin polarized<sup>3,4,5,6,7,8,9</sup> ground state. This ground state is characterized by opposite spin orientations of localized electronic states at the two edges of the GNR, which couple through the graphene backbone via an antiferromagnetic (AF) arrangement of spins on adjacent atomic sites.

In a recent study, Son *et al.*<sup>9</sup> have shown that upon the application of an electric field, an opposite local gating effect of the spin states on the two edges of the ribbon may occur. The in-plane field (perpendicular to the periodic axis of the ribbon) drives the system into a half-metallic

state where one spin flavor exhibits metallic behavior, while the opposite experiences an increase in the energy gap. Chemical doping of the ribbon edges was shown to enhance this effect resulting in an efficient and robust spin filter device.<sup>21</sup>

Following these studies on the half-metallic nature of *one-dimensional* zigzag graphene nanoribbons, several papers on the electronic properties,<sup>22</sup> magnetic properties<sup>23,24,25,26</sup> and the half-metallic nature<sup>27,28</sup> of *quasi-zero-dimensional* graphene-based structures have appeared. These concluded that the spin polarized character of the zigzag graphene edges persists also in nanometer scale islands of graphene, and that the half-metallic nature of the structures studied by Son *et al.*<sup>9</sup> may be an artifact of the level of theory they applied.<sup>27</sup>

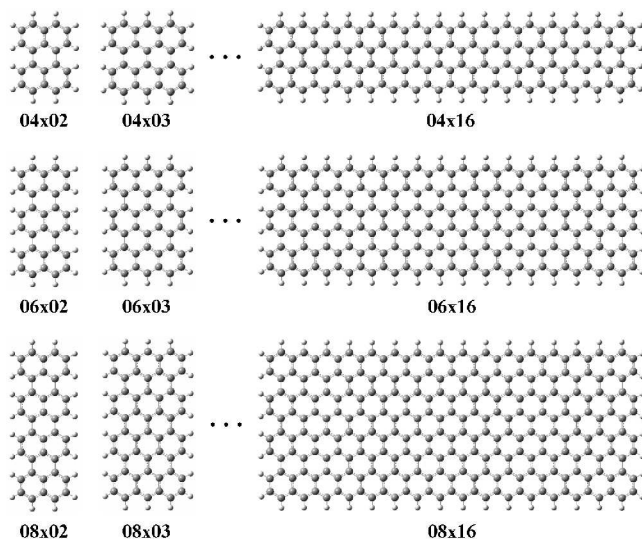


FIG. 1: The three sets of finite GNRs studied. The notation corresponds to the number of hydrogen atom passivating the edges. A  $N \times M$  ribbon has  $N$  hydrogens on the armchair edge and  $M$  hydrogens on the zigzag edge.

It is the purpose of our paper to present a comprehensive and systematic analysis of the electronic properties of finite-sized graphene nanoribbons. We present a general rule of thumb for the existence of a spin-polarized ground state in aromatic carbon based materials and identify the molecules  $C_{28}H_{14}$  (Phenanthro[1,10,9,8-opqra]perylene) and  $C_{36}H_{16}$  (Tetrabenzo[bc,ef,kl,no]coronene) as the smallest hydrocarbon structures to possess a magnetic ground state. The stability of the magnetic ordering, the energy gap dependence on the dimensions of the system, and the effect of an externally applied electric field are also studied. Unlike previous studies,<sup>27</sup> we show that the half-metallic nature of the ribbons (whether periodic or finite) is robust and insensitive to the level of theory used.

To this end we study a large set of finite rectangular nanoribbons of different widths and lengths using three levels of density functional approximations. We notate the ribbons according to the number of hydrogen atoms passivating the edges, such that a  $N \times M$  finite ribbon has  $N$  hydrogen atoms on its armchair edge and  $M$  atoms on its zigzag edge (see Fig. 1). The ribbons we consider constitute three sub-sets corresponding to three ribbon widths:  $4 \times M$ ,  $6 \times M$ , and  $8 \times M$ , where  $M = 2, \dots, 16$ . All the calculations presented in this work were carried out using the development version of the *Gaussian* suite of programs.<sup>29</sup> Spin polarized ground state calculations were performed using the local density approximation<sup>30</sup> (LDA), the semi-local gradient corrected functional of Perdew, Burke and Ernzerhof<sup>30,31,32</sup> (PBE), and the screened exchange hybrid density functional due to Heyd, Scuseria and Ernzerhof (HSE06),<sup>30,33,34,35</sup> which has been tested in a wide variety of materials and has been shown to accurately reproduce experimental band gaps<sup>36,37</sup> and first and second optical excitation energies in metallic and semiconducting single walled CNTs.<sup>38,39</sup> The inclusion of short-range exact-exchange in the HSE06 functional makes it suitable to treat electronic localization effects<sup>40,41,42,43,44</sup> which are known to be important in this type of materials.<sup>3,4,5,6,7,8,9,16,20,21,45,46,47,48,49,50,51,52,53</sup> This is further supported by the good agreement which was recently obtained between predicted bandgaps<sup>15</sup> of narrow nanoribbons and measured values.<sup>17</sup> To obtain a reliable ordering of the different magnetization states we find it important to relax the geometry of the finite GNRs for each spin polarization. Therefore, unless otherwise stated, all reported electronic properties are given for fully optimized structures for each approximate functional using the polarized 6-31G\*\* Gaussian basis set.<sup>54</sup> It should be noted that since our calculations are performed within a single determinantal framework, we can determine only the total spin vector projection along a given axis  $m_s$  and not the total spin.

Given that most organic molecules are known to be diamagnetic, while periodic<sup>3,4,5,6,7,8,9,21</sup> and finite graphene clusters<sup>23,24,25,27</sup> are predicted to have a spin polarized ground state, we begin by studying the emer-

gence of magnetic ordering in ultra-short and ultra-narrow rectangular graphene nanoribbons. In panels (a)-(e) of Fig. 2 we present the ground state spin density of representative structures of each of the subsets studied as obtained using the HSE06 density functional. All the structures studied have compensated lattices in the sense that the number of carbon atoms belonging to each graphene sub-lattice are balanced. Therefore, according to Lieb's theorem for bipartite lattices<sup>25,55</sup> they have no total spin moment. The two smallest structures that present magnetic ordering in their ground state are found to be the Phenanthro[1,10,9,8-opqra]perylene (bisanthrene) isomer of the  $C_{28}H_{14}$  molecule and the Tetrabenzo[bc,ef,kl,no]coronene isomer of the  $C_{36}H_{16}$  molecule. The later was recently identified as spin polarized using gradient corrected and hybrid density functionals.<sup>26</sup> This is a remarkable finding regarding the expected aromatic hydrocarbon nature of these two isomers especially in light of a previous study that predicted the ground state to be diamagnetic and the first excited state to be of diradical nature (see panel (f) of Fig. 2).<sup>56</sup> Hence, our HSE06 results suggest that the energy gain from the antiferromagnetic ordering of spins obtained in the hexaradical Clar structure (see panel (g) of Fig. 2) is higher than the aromatic stabilization even for this small organic molecule.

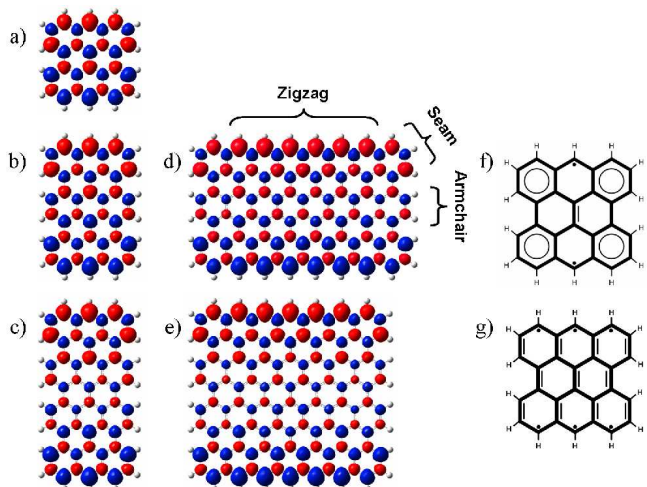


FIG. 2: Isosurface spin densities of the antiferromagnetic ground state of the 04x03 (panel (a)), 06x03 (panel (b)), 08x03 (panel (c)), 06x08 (panel (d)), and 08x07 (panel (e)) GNRs as obtained using the HSE06 functional and the 6-31G\*\* basis set. The sorting of the atoms into zigzag, armchair and seam regions is indicated in panel (d). Panels (f) and (g) represent the diradical and hexaradical Clar structures of bisanthrene

From a qualitative analysis of the spin density maps we conclude that the edge atoms can be divided into three subgroups: atoms which distinctly belong to a zigzag edge, atoms that distinctly belong to an armchair edge, and atoms belonging to the seam region between the

two types of edges (see panel (d) of Fig.2). As a rule

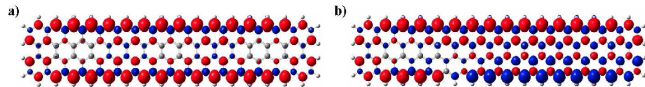


FIG. 3: Spin density isosurfaces of the  $04 \times 16$  GNR high spin multiplicity states as obtained at the PBE/6-31G\*\* level of theory. Panel (a): ferromagnetic arrangement of the  $m_s = 3$  state. Panel (b): mixed configuration of the  $m_s = 1$  state presenting a short spin wave on one of the zigzag edges.

of thumb we find that for rectangular ribbons of width  $N = 4$  and above, every carbon atom that distinctly belongs to a zigzag edge will be spin polarized. Seam region edge atoms will have a lower spin polarization, while edge atoms on a pure armchair edge are considerably less polarized. Therefore, the  $N \times 2$  structures, which have no distinct zigzag edge atoms show a diamagnetic ground state, while the  $N \times 3$  (and longer) structures have magnetic ordering in their ground state.

An interesting finding is the fact that the maximum Mulliken spin polarization on the zigzag edge carbon atoms seems to be approximately constant for all the systems studied and depends mostly on the density functional chosen. For the local density approximation this value is usually between 0.26 and 0.30, whereas the maximum Mulliken spin density is within 0.30 – 0.37 at the PBE level of theory. For the HSE functional, the range is 0.40 – 0.47. A second important conclusion is that for the short systems ( $3 \lesssim M \lesssim 8$ ) the energetic ordering of the spin states is  $E_{\uparrow\downarrow} < E_{\uparrow\uparrow} < E_0$ . Here  $E_{\uparrow\downarrow}$  is the total energy of the antiferromagnetic ground state (Fig. 2),  $E_{\uparrow\uparrow}$  is the energy of the ferromagnetic arrangement with a total spin moment projection of  $m_s = 1$  and parallel spins on both zigzag edges (see panel (a) of Fig. 3), and  $E_0$  is the total energy of the diamagnetic state. For longer ribbons, while the ground state remains antiferromagnetic, the above lying state is not necessarily the  $m_s = 1$  state anymore. The number unpaired electrons is not sufficient to sustain the desired maximum spin polarization on the zigzag edges while maintaining the ferromagnetic ordering. Instead, a mixed configuration is obtained where both spin polarizations appear on the same ribbon edge forming a type of a short spin wave (see panel (b) of Fig. 3). As a result the energy of the  $m_s = 1$  state is raised, usually above the  $m_s = 2$  state, which in turn becomes the lowest energy state with finite total spin.

To quantify these findings we study the stability of the antiferromagnetically ordered ground state with respect to the above lying higher spin multiplicity state. In Fig. 4 the energy differences between the antiferromagnetic ground state and the first higher spin multiplicity state are presented for the three sets of ribbons studied. All diagrams are characterized by sharp maxima structures that correspond to the ribbon length at which a transition in the magnetization nature of the first higher spin state occurs, as discussed above. We note

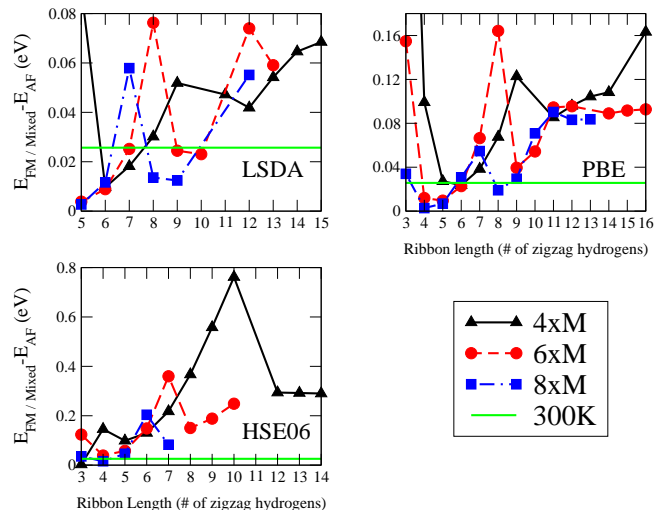


FIG. 4: Energy differences between the antiferromagnetic (AF) ground state and the above lying higher spin multiplicity ferromagnetic (FM) or mixed state for the three sets of ribbons studied as calculated by the local spin density approximation (upper left panel), PBE functional (upper right panel), and the HSE06 functional (lower left panel). The green line represents  $k_B T$  at room temperature. Notice the different energy scales obtained for the different functional calculations.

that even though the antiferromagnetic state of  $04 \times 03$  (bisanthrene), as calculated at the HSE06 level of theory, is only 0.003eV (30K) below the above lying ferromagnetic state, the  $04 \times 04$  structure has an energy difference of  $\sim 0.15$ eV (1700K), suggesting the detectability of its magnetic ordering even at room temperature. Furthermore, the HSE06 results indicate considerably large energy differences between the antiferromagnetic ground state and higher spin states for all ribbons with  $N \geq 4$  and length exceeding 1nm.

Before discussing the effect of an electric field on the electronic properties of finite nanoribbons, it is essential to study their ground state characteristics in the absence of external perturbations. The geometry dependence of the HOMO-LUMO (highest occupied molecular orbital and lowest unoccupied molecular orbital, respectively) gap would be the most important parameter to address. In Fig. 5 the energy gap as a function of the length of the ribbon are presented, for the three subsets of ribbons considered and the three density functional approximations used. Even though up to now we have regarded the studied structures as zigzag nanoribbons, one can also think of them as wide and short armchair ribbons due to their finite length. These type of ribbons are known to present remarkable bandgap oscillations as a function of the ribbon width<sup>14,15</sup> for infinitely long armchair GNRs. Such oscillations can be clearly seen in Fig. 5 especially for the PBE results (upper right panel). The periodicity of the oscillation appears to be somewhat different than the threefold period obtained for the infinitely long counter-

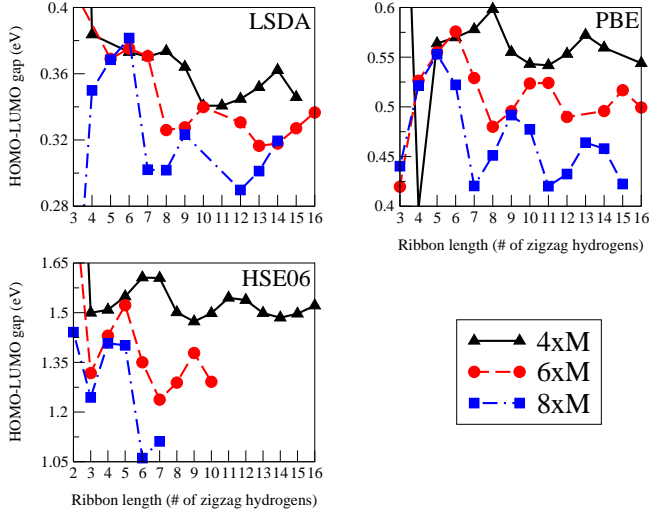


FIG. 5: HOMO-LUMO gap values for the three sets of ribbons studied as calculated by the local spin density approximation (upper left panel), PBE functional (upper right panel), and the HSE06 functional (lower left panel). Notice the different energy scales obtained for the different functionals calculations.

parts. This, however, is a result of the fact that in order to prevent dangling carbon bonds, the width step taken for the finite systems is twice that taken in the infinitely long armchair ribbon calculations. The amplitude of the oscillations is found to be considerably damped due to the finite size of the ribbons in agreement with a previous study.<sup>23</sup> As expected, when the length of the armchair edge ( $N$ ) is increased, the oscillations amplitude increases as well. It is interesting to note that, in general, the HOMO-LUMO gap is inversely proportional to the width ( $N$ ) and the length ( $M$ ) of the finite GNR in accordance with the semi-metallic graphene sheet limit. Therefore, in order to obtain energy gap tailoring capability one will have to consider GNRs with long armchair edges (large  $N$  values) and short zigzag edges (small  $M$  values). This will increase the amplitude of the energy gap oscillations while maintaining overall higher gap values.

Having explored the electronic properties of unperturbed finite GNRs, we now turn to discuss the answer to the main question addressed in this study, namely, will finite nanoribbons turn half-metallic under the influence of an external electric field? In a previous study, it was argued that the inclusion of Hartree-Fock exchange in the approximate density functional results in the disappearance of the half metallic state.<sup>27</sup> This was shown to be not true in periodic systems where screened exchange (and unpublished full exact exchange) calculations have shown half-metallic behavior similar to that obtained with semi-local and gradient corrected functionals.<sup>21</sup> In Fig. 6 we present the spin-polarized HOMO-LUMO gap dependence on an external in-plane electric

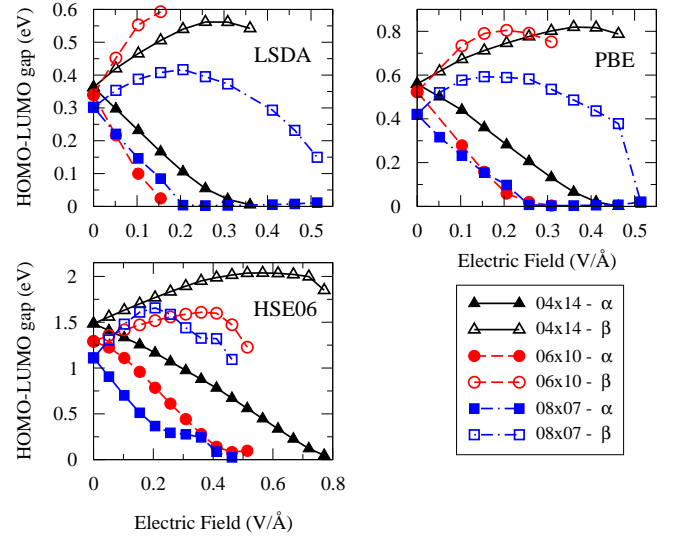


FIG. 6: Spin-polarized HOMO-LUMO gap dependence on the strength of an external in-plane electric field for three representative finite nanoribbons as calculated by the local spin density approximation (upper left panel), PBE functional (upper right panel), and the HSE06 functional (lower left panel). Fixed geometries of the relaxed structures in the absence of the external field at each level of theory were used. Notice the different energy scales obtained for the different functionals calculations.

field applied perpendicular to the zigzag edge, for three representative finite GNRs. Similar to previous calculations for periodic systems,<sup>9,21</sup> in the absence of an external field the  $\alpha$  and  $\beta$  gaps are degenerate. Upon the application of the field, electrons having one spin flavor experience a smooth increase in the HOMO-LUMO gap while the opposite spin flavor experiences a decrease in the gap. This gap splitting continues up to a point where the decreased gap vanishes creating a degenerate zero energy state. As expected, wider systems require a lower onset field to obtain this half-metallic state.<sup>9</sup> At this point, due to the increased mobility of the metallic electrons, further increase in the external field results in spin transfer between both edges thus reducing the total spin polarization and the energy gap splitting. At higher electric fields the systems become diamagnetic.<sup>21,28</sup> All three representative structures present the same features described above. The main difference between the LSDA, PBE and HSE06 results is the zero-field HOMO-LUMO gap, and thus the onset electric field required to induce half-metallic behavior. Nevertheless, they all predict the appearance of the half-metallic state at an appropriate electric field strength.

To summarize, we have presented a detailed study of the electronic properties of finite rectangular graphene nanoribbons. Bisanthrene is predicted to be the smallest organic hydrocarbon structure to present a spin polarized ground state. This state is characterized with antiferromagnetic ordering of spins at the to zigzag edges

of the molecule. As a rule of thumb we find that zigzag edges, that are at least three consecutive units long, will present spin polarization if the width of the system is 1 nm or wider. For systems with zigzag edges 1 nm and longer, our HSE06 results predict the antiferromagnetic ordering to be considerably stable with respect to higher spin multiplicity states, suggesting the room temperature detectability of their spin polarization. Depending on the dimensions of the system higher spin states can have antiferromagnetic ordering or be of mixed nature with spin wave characteristics. Similar to periodic ribbons, HOMO-LUMO gap oscillations with the length of the zigzag edge are observed. The amplitude of these

oscillations however, is lower than that predicted for infinite ribbons. The half-metallic nature of the ribbons under an external in-plane electric field is preserved even for finite and extremely short GNRs, regardless of the level of theory used.

## Acknowledgments

This work was supported by NSF Award Number CHE-0457030 and the Welch Foundation. Calculations were performed in part on the Rice Terascale Cluster funded by NSF under Grant EIA-0216467, Intel, and HP. O.H. would like to thank the generous financial support of the Rothschild and Fulbright foundations.

- <sup>1</sup> K. S. Novoselov, A. K. Geim, S. V. Morozov, D. Jiang, Y. Zhang, S. V. Dubonos, I. V. Grigorieva, and A. A. Firsov, *Science* **306**, 666 (2004).
- <sup>2</sup> C. Berger, Z. Song, X. Li, X. Wu, N. Brown, C. Naud, D. Mayou, T. Li, J. Hass, A. N. Marchenkov, E. H. Conrad, P. N. First, and W. A. de Heer, *Science* **312**, 1191 (2006).
- <sup>3</sup> M. Fujita, K. Wakabayashi, K. Nakada, and K. Kusakabe, *J. Phys. Soc. Jap.* **65**, 1920 (1996).
- <sup>4</sup> K. Wakabayashi, M. Sigrist, and M. Fujita, *J. Phys. Soc. Jap.* **67**, 2089 (1998).
- <sup>5</sup> K. Wakabayashi, M. Fujita, H. Ajiki, and M. Sigrist, *Phys. Rev. B* **59**, 8271 (1999).
- <sup>6</sup> K. Kusakabe and M. Maruyama, *Phys. Rev. B* **67**, 092406 (2003).
- <sup>7</sup> A. Yamashiro, Y. Shimoi, K. Harigaya, and K. Wakabayashi, *Phys. Rev. B* **68**, 193410 (2003).
- <sup>8</sup> H. Lee, Y.-W. Son, N. Park, S. Han, and J. Yu, *Phys. Rev. B* **72**, 174431 (2005).
- <sup>9</sup> Y.-W. Son, M. L. Cohen, and S. G. Louie, *Nature* **444**, 347 (2006).
- <sup>10</sup> Y. Zhang, Y.-W. Tan, H. L. Stormer, and P. Kim, *Nature* **438**, 201 (2005).
- <sup>11</sup> N. M. R. Peres, A. H. Castro-Neto, and F. Guinea, *Phys. Rev. B* **73**, 195411 (2006).
- <sup>12</sup> N. M. R. Peres, A. H. Castro-Neto, and F. Guinea, *Phys. Rev. B* **73**, 241403 (2006).
- <sup>13</sup> K. S. Novoselov, Z. Jiang, Y. Zhang, S. V. Morozov, H. L. Stormer, U. Zeitler, J. C. Maan, G. S. Boebinger, P. Kim, and A. K. Geim, *Science* **315**, 1379 (2007).
- <sup>14</sup> M. Ezawa, *Phys. Rev. B* **73**, 045432 (2006).
- <sup>15</sup> V. Barone, O. Hod, and G. E. Scuseria, *Nano Lett.* **6**, 2748 (2006).
- <sup>16</sup> Y.-W. Son, M. L. Cohen, and S. G. Louie, *Phys. Rev. Lett.* **97**, 216803 (2006).
- <sup>17</sup> M. Y. Han, B. Özyilmaz, Y. Zhang, , and P. Kim, *Phys. Rev. Lett.* **98**, 206805 (2007).
- <sup>18</sup> R. Saito, G. Dresselhaus, and M. S. Dresselhaus, *Physical Properties of Carbon Nanotubes* (Imperial College Press, London, 1998).
- <sup>19</sup> M. S. Dresselhaus, G. Dresselhaus, and P. Avouris, *Topics in Applied Physics, Vol. 80* (Springer, Heidelberg, 2001).
- <sup>20</sup> K. Nakada, M. Igami, and M. Fujita, *J. Phys. Soc. Jap.* **67**, 2388 (1998).
- <sup>21</sup> O. Hod, V. Barone, J. E. Peralta, and G. E. Scuseria, *Nano Lett.* **7**, 2295 (2007).
- <sup>22</sup> P. G. Silvestrov and K. B. Efetov, *Phys. Rev. Lett.* **98**, 016802 (2007).
- <sup>23</sup> P. Shemella, Y. Zhang, M. Mailman, P. M. Ajayan, and S. K. Nayak, *Appl. Phys. Lett.* **91**, 042101 (2007).
- <sup>24</sup> M. Ezawa, arXiv:0707.0349v1 [cond-mat.mes-hall].
- <sup>25</sup> J. Fernandez-Rossier, J. J. Palacios, arXiv:0707.2964v1 [cond-mat.mes-hall].
- <sup>26</sup> De-en Jiang, Bobby G. Sumpter, Sheng Dai, arXiv:0706.0863v2 [physics.chem-ph].
- <sup>27</sup> E. Rudberg, P. Salek, and Y. Luo, *Nano Lett.* **7**, 2211 (2007).
- <sup>28</sup> Er-Jun Kan, Zhenyu Li, Jinlong Yang, J. G. Hou, arXiv:0708.1213v1 [physics.mtrl-sci Materials Science].
- <sup>29</sup> Frisch, M. J. et al., Gaussian, Inc., Pittsburgh, PA, *Gaussian Development Version, Revision E.05* (2003).
- <sup>30</sup> The local density, gradient corrected, and screened hybrid approximations are obtained using the SVWN5, PBEPE, and HSE1PBE keywords in *Gaussian*, respectively.
- <sup>31</sup> J. P. Perdew, K. Burke, and M. Ernzerhof, *Phys. Rev. Lett.* **77**, 3865 (1996).
- <sup>32</sup> J. P. Perdew, K. Burke, and M. Ernzerhof, *Phys. Rev. Lett.* **78**, 1396 (1997).
- <sup>33</sup> J. Heyd, G. E. Scuseria, and M. Ernzerhof, *J. Chem. Phys.* **118**, 8207 (2003).
- <sup>34</sup> J. Heyd, G. E. Scuseria, and M. Ernzerhof, *J. Chem. Phys.* **124**, 219906 (2006).
- <sup>35</sup> A. F. Izmaylov, G. E. Scuseria, and M. J. Frisch, *J. Chem. Phys.* **125**, 104103 (2006).
- <sup>36</sup> J. Heyd and G. E. Scuseria, *J. Chem. Phys.* **121**, 1187 (2004).
- <sup>37</sup> J. Heyd, J. E. Peralta, and G. E. Scuseria, *J. Chem. Phys.* **123**, 174101 (2005).
- <sup>38</sup> V. Barone, J. E. Peralta, M. Wert, J. Heyd, and G. E. Scuseria, *Nano Lett.* **5**, 1621 (2005).
- <sup>39</sup> V. Barone, J. E. Peralta, and G. E. Scuseria, *Nano Lett.* **5**, 1830 (2005).
- <sup>40</sup> K. N. Kudin, G. E. Scuseria, and R. L. Martin, *Phys. Rev. Lett.* **89**, 266402 (2002).
- <sup>41</sup> I. D. Prodan, J. A. Sordo, K. N. Kudin, G. E. Scuseria, and R. L. Martin, *J. Chem. Phys.* **123**, 014703 (2005).
- <sup>42</sup> I. D. Prodan, G. E. Scuseria, and R. L. Martin, *Phys. Rev. B* **73**, 045104 (2006).
- <sup>43</sup> P. J. Hay, R. L. Martin, J. Uddin, and G. E. Scuseria, *J. Chem. Phys.* **125**, 034712 (2006).
- <sup>44</sup> D. Kasinathan, J. Kunes, K. Koepernik, C. V. Diaconu,

- R. L. Martin, I. D. Prodan, G. E. Scuseria, N. Spaldin, L. Petit, T. C. Schulthess, and W. E. Pickett, *Phys. Rev. B* **74**, 195110 (2006).
- <sup>45</sup> K. Kobayashi, *Phys. Rev. B* **48**, 1757 (1993).
- <sup>46</sup> K. Nakada, M. Fujita, G. Dresselhaus, and M. S. Dresselhaus, *Phys. Rev. B* **54**, 17954 (1996).
- <sup>47</sup> Y. Miyamoto, K. Nakada, and M. Fujita, *Phys. Rev. B* **59**, 9858 (1999).
- <sup>48</sup> T. Kawai, Y. Miyamoto, O. Sugino, and Y. Koga, *Phys. Rev. B* **62**, 16349 (2000).
- <sup>49</sup> S. Okada and A. Oshiyama, *Phys. Rev. Lett.* **87**, 146803 (2001).
- <sup>50</sup> Y. Niimi, T. Matsui, H. Kambara, K. Tagami, M. Tsukada, and H. Fukuyama, *Appl. Surf. Sci.* **241**, 43 (2005).
- <sup>51</sup> Y. Kobayashi, K. ichi Fukui, T. Enoki, K. Kusakabe, and Y. Kaburagi, *Phys. Rev. B* **71**, 193406 (2005).
- <sup>52</sup> Y. Niimi, T. Matsui, H. Kambara, K. Tagami, M. Tsukada, and H. Fukuyama, *Phys. Rev. B* **73**, 085421 (2006).
- <sup>53</sup> Y. Kobayashi, K. ichi Fukui, T. Enoki, and K. Kusakabe, *Phys. Rev. B* **73**, 125415 (2006).
- <sup>54</sup> P. C. Hariharan and J. A. Pople, *Theoret. Chimica Acta* **28**, 213 (1973).
- <sup>55</sup> E. H. Lieb, *Phys. Rev. Lett.* **62**, 1201 (1989).
- <sup>56</sup> J. R. Dias, *J. Chem. Inf. Model.* **46**, 788 (2006).